

# On the Mechanism of Divalent Metal Ion Chelator Induced Activation of the 7S Nerve Growth Factor Esteropeptidase. Activation by 2,2',2''-Terpyridine and by 8-Hydroxyquinoline-5-sulfonic acid†

Scott E. Pattison† and Michael F. Dunn\*

**ABSTRACT:** Our previous studies (Pattison, S. E., and Dunn, M. F. (1975), *Biochemistry* 14, 2733) have shown that the reaction of divalent metal ion chelators with the 140 000 mol wt mouse submaxillary nerve growth factor protein (7S NGF) activates the  $\gamma$ -subunit esteropeptidase activity ca. sevenfold. Ultraviolet-visible spectral studies with the chelator 2,2',2''-terpyridine (terpyridine) and fluorescence emission studies with 8-hydroxyquinoline-5-sulfonic acid (HQSA) in combination with both conventional and rapid-mixing stopped-flow kinetic techniques have been employed in the present study to investigate (a) the mechanism of the chelator-induced activation process, and (b) the identity of the divalent metal ion involved. The spectral studies confirm the presence of stoichiometrically significant amounts of tightly bound zinc ion in native 7S NGF (1–2 g-atoms of  $\text{Zn}^{2+}$ /mol of 7S NGF). The kinetic studies show that the reaction of terpyridine with 7S NGF occurs via a two-step process in-

volving first a rapid, apparent second-order step ( $k_1 = 1 \times 10^6 \text{ M}^{-1} \text{ s}^{-1}$ ) to form a 7S NGF- $\text{Zn}^{2+}$ -chelator monocomplex, then a slow step to form a bis(terpyridine)- $\text{Zn}(\text{II})$  complex and activated 7S NGF in an apparent first-order process ( $k_{\text{obsd}} = 0.10 \text{ min}^{-1}$ ). This rate is, within experimental error, identical with the apparent first-order rate constant for the chelator-induced activation process (monitored by the rate of change in the steady-state rate of hydrolysis of chromophoric substrate,  $\alpha$ -N-benzoyl-D,L-arginine-p-nitroanilide). Kinetic studies of the reaction of HQSA with native 7S NGF show that, under the same conditions of concentration, the rate of formation of the tris(HQSA)- $\text{Zn}(\text{II})$  complex is identical with the rate of the HQSA-induced activation of the 7S NGF esteropeptidase. Thus, these studies unambiguously establish that zinc ion is the metal ion involved in the chelator-induced activation process, and that activation involves removal of zinc ion from native 7S NGF.

The mouse submaxillary nerve growth factor protein (NGF)<sup>1</sup> both enhances and regulates the in vivo growth and differentiation of two neural crest derivatives, the noradrenergic neurons of the superior cervical ganglia and the sensory neurons of the dorsal root ganglia (Cohen, 1960; Levi-Montalcini, 1966; Schenkein, 1972). The nerve growth promoting protein (2.5S NGF or  $\beta$ ) is isolated at neutrality as a 140 000 mol wt (7S) oligomer associated with two other protein classes (designated  $\alpha$ ,  $\gamma$ ) (Varon et al., 1967). The three protein classes ( $\alpha$ ,  $\beta$ , and  $\gamma$ ) appear to interact both tightly and specifically (Perez-Polo et al., 1972). However, the 7S oligomer possesses an in vitro growth-promoting activity approximately equivalent to that of the isolated  $\beta$ -subunit. Thus, the function of 7S NGF in the regulation of neuronal growth and differentiation (as measured by the in vitro organ culture assay) is open to speculation.

The 7S NGF  $\gamma$ -subunit possesses a trypsin-like esteropeptidase activity. This activity is nearly completely suppressed in the native oligomer (Greene et al., 1969). The specific physical association of the  $\gamma$ -esteropeptidase subunit and the

growth-promoting subunit within the oligomer (Moore et al., 1974) implies a functional interrelationship. Therefore, it is probable that this form of the complex is not the physiologically functional form of the protein.

Based on the finding that the C-terminus of the  $\beta$ -subunit is an Arg residue, Frazier et al. (1972) and Moore et al. (1974) have suggested that the role of the  $\gamma$ -esteropeptidase is to convert a "pro- $\beta$ " to the active peptide ( $\beta$ ). Moore et al. (1974) have reported that the des-Arg derivative of  $\beta$  is incapable of forming a 7S oligomer when mixed with the  $\alpha$  and  $\gamma$  subunits. Hence, they suggest that binding of the C-terminal Arg of  $\beta$  to the active site of  $\gamma$  is critical to the stability of the oligomer, and that this interaction accounts for the suppressed proteolytic activity of the native 7S oligomer.

Recently, we have reported evidence suggesting that 7S NGF is a zinc metalloprotein (Pattison and Dunn, 1975). Zinc ion was also shown to be a specific inhibitor of the  $\gamma$ -esteropeptidase activity ( $K_i \approx 8 \times 10^{-7} \text{ M}$ ). Finally, divalent metal ion chelators were shown to elicit a sevenfold increase in esteropeptidase activity in 7S NGF solutions.

This paper presents a study of the interaction between 7S NGF and the chelators, 2,2',2''-terpyridine (terpyridine) and 8-hydroxyquinoline-5-sulfonic acid (HQSA). We show: (1) that zinc ion is the metal ion involved in the chelator-induced activation of the 7S NGF esteropeptidase, and (2) that activation and loss of zinc ion from the protein are concomitant processes. The kinetics and thermodynamics of the activation reaction are presented in the following paper in this issue.

## Materials and Methods

Both 7S NGF (Varon et al., 1967) and the 7S NGF subunits (Smith et al., 1968) were isolated according to published

† From the Department of Biochemistry, University of California, Riverside, California, 92502. Received October 10, 1975. Supported by American Cancer Society Grants DT-4 (National Division) and 544 (California Division), and by funds from the University of California Cancer Research Coordinating Committee.

\* Present address: Institute of Molecular Biology, University of Oregon, Eugene, Oregon, 97403. This work was carried out in partial fulfillment of the requirements for the Ph.D. degree and formed part of the dissertation.

<sup>1</sup> Abbreviations used are: 7S NGF, mouse submaxillary nerve growth factor protein; HQSA, 8-hydroxyquinoline-5-sulfonic acid; Tris, 2-amino-2-hydroxymethyl-1,3-propanediol; uv, ultraviolet; EDTA, (ethylenedinitrilo)tetraacetic acid; BAPNA,  $\alpha$ -N-benzoyl-D,L-arginine-p-nitroanilide.

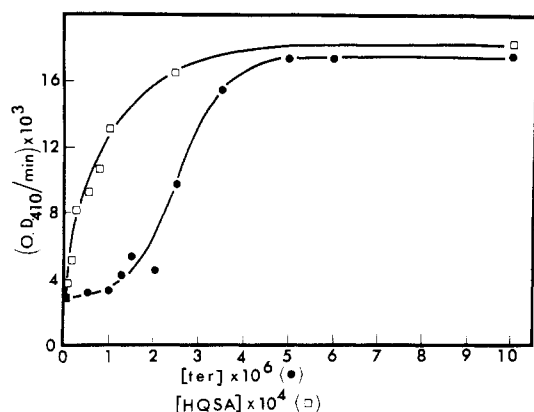


FIGURE 1: The dependence of the extent of 7S NGF esterase activation on the concentration of divalent metal ion chelator ((●) 2,2',2''-terpyridine, (□) 8-hydroxyquinoline-5-sulfonic acid). A concentration of  $\sim 0.2 \mu\text{M}$  7S NGF was incubated in 0.05 M Tris buffer, pH 7.4, with the chelator at room temperature for at least 1 h prior to initiation of the esterase assay. The steady-state esterase activity was assayed by measuring the hydrolysis rate ( $v$ ) on addition of a 10- $\mu\text{l}$  aliquot of the artificial substrate  $\alpha$ -N-benzoyl-D,L-arginine-p-nitroanilide (final concentration, 1 mM).

procedures and as described in our previous paper (Pattison and Dunn, 1975). Both the 7S NGF and the  $\beta$ -subunit preparations were found to have in vitro growth-promoting activities that are comparable to those previously reported (Varon et al., 1967; Smith et al., 1968) when assayed with the organ culture procedure of Levi-Montalcini and Hamburger (1953).

Equilibrium and slow kinetic uv-visible spectral studies were made either on a Cary 118c spectrophotometer or a Varian 635 uv-visible spectrophotometer at  $25.0 \pm 0.2^\circ\text{C}$  upon mixing chelator with either 7S NGF or a divalent metal ion. The fluorescence studies were made with a Farrand MK-I recording spectrofluorometer. Cuvettes were prepared by presoaking for 30 min with concentrated hydrochloric acid followed by a double-distilled water wash to decrease divalent metal ion contamination. Equilibrium measurements were made after incubating the assay mixtures for approximately 90 min at room temperature in the assay cuvette. Kinetic measurements of slow reactions were initiated by an addition of a 10- $\mu\text{l}$  aliquot of chelator stock solution to a cuvette containing 7S NGF in 0.05 M Tris buffer, pH 7.4. Stopped-flow, rapid-mixing kinetic measurements were made on a Durrum D-110 spectrophotometer at  $25.0 \pm 0.5^\circ\text{C}$ . The glass storage syringes and mixing chamber were washed with 10  $\mu\text{M}$  EDTA, followed by a wash with Chelex resin-treated buffer in order to minimize divalent metal ion contamination.

The total metal content of a 7S NGF preparation in 0.05 M Tris buffer, pH 7.4, was determined using a Tarrell-Ash 3.4-m direct-reading emission spectrograph. The 7S NGF sample was prepared by first oxidizing all organic material. The remaining inorganic salts were then redissolved and ignited in an electric arc. The metal ion concentrations were determined by measuring spectral line intensities.

The 7S NGF esterase activity was determined from the rate of hydrolysis of the chromophoric substrate,  $\alpha$ -N-benzoyl-D,L-arginine-p-nitroanilide (BAPNA) (Sigma Chemical Co.) at  $25.0 \pm 0.2^\circ\text{C}$  in 0.05 M Tris buffer, pH 7.4.

## Results

*Comparison of Spectral Changes with Activity Changes upon Chelator-7S NGF Interaction.* As reported in the fol-

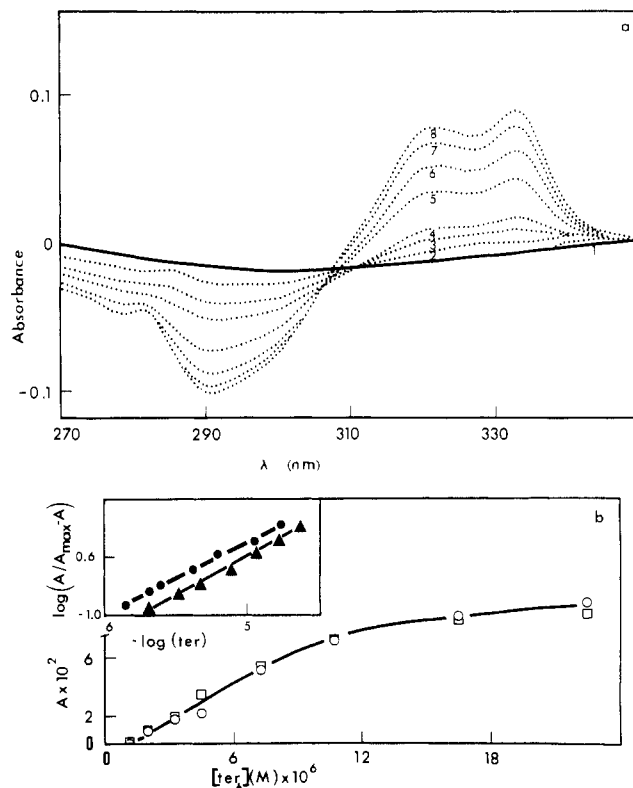


FIGURE 2: (a) The variation in double-difference spectra produced by successive additions of 2,2',2''-terpyridine to a solution containing 7S NGF. Each spectrum was measured after the 7S NGF-terpyridine solution ( $\sim 2 \mu\text{M}$ ) had been incubated at room temperature for 90 min. Identical 10- $\mu\text{l}$  aliquots of terpyridine were added to both the sample and reference cells. The final terpyridine concentrations were as follows: (1) 0.8  $\mu\text{M}$ ; (2) 3  $\mu\text{M}$ ; (3) 4.2  $\mu\text{M}$ ; (4) 5.4  $\mu\text{M}$ ; (5) 8.4  $\mu\text{M}$ ; (6) 11.4  $\mu\text{M}$ ; (7) 71.4  $\mu\text{M}$ ; (8) 0.130 mM. The spectra were scanned on a Cary 118c spectrophotometer at 0.2 nm/s. In order to correct for protein absorbance, the reference cell also contained 7S NGF in one compartment of the split cuvette. (b) The concentration dependence of the 2,2',2''-terpyridine spectral changes produced by 7S NGF interaction with the chelator. The plot in a shows the absolute variation in  $A_{290}$  (□) and  $A_{332}$  (○) vs. the total terpyridine concentration ( $\text{ter}_t$ ) added to an approximately  $2 \mu\text{M}$  7S NGF solution buffered with 0.05 M Tris buffer, pH 7.4 at  $25.0 \pm 0.2^\circ\text{C}$ . The inset to this figure is a plot of the  $\log [(A_{332})/(A_{332\text{max}} - A_{332})]$  vs. either the log of the total terpyridine concentration (▲) or the log of the difference between the total terpyridine concentration and the approximate concentration of bound terpyridine (as calculated from the measured disappearance of free terpyridine,  $\epsilon_{290} = 1.6 \times 10^4 \text{ M}^{-1} \text{ cm}^{-1}$ , Hoyer et al., 1966) (●), according to the method of Hill (Barcroft and Hill, 1909). Optical density measurements were performed with a Cary 118c spectrophotometer.

lowing paper, incubation of 7S NGF with a wide variety of divalent metal ion chelators activates the 7S NGF esterase to the same final catalytic activity independent of the chelator structure, provided the chelator concentration is sufficiently high. However, over the range of chelators examined, the concentration dependence of activation shows varying degrees of sigmoidal character. The terpyridine activation isotherm (Figure 1) is sigmoidal with a Hill coefficient of  $2.6 \pm 0.5$ , whereas the HQSA isotherm is essentially hyperbolic with a Hill coefficient of  $1.2 \pm 0.2$ .

The spectral changes that accompany the terpyridine-7S NGF reaction provide a convenient means for directly examining the interactions between chelator and 7S NGF that culminate in activation. The spectral changes that take place during a typical terpyridine titration of 7S NGF are shown in Figure 2. These difference spectra show that at low chelator concentrations a new (minor) species absorbing at approximately 341 nm is observed. Subsequent additions of terpyridine

give a second (major) species exhibiting maxima at  $321.5 \pm 0.5$  and  $332.5 \pm 0.5$  nm and a minimum at approximately 290 nm. These difference-spectra titrations do not exhibit a true isosbestic point. However, the deviation from isosbesticity is slight, and it appears that free terpyridine and the  $321.5$ – $332.5$  nm absorbing terpyridine complex are the two principal species in solution over the concentration range investigated.

Measurements of the absorbance changes at 332 nm as a function of increasing terpyridine concentration show an increase that follows a sigmoidal isotherm with a Hill coefficient of  $2.06 \pm 0.3$  (Figure 2b). When this process is monitored at 290 nm, the wave length of absorbance for free terpyridine, the decrease in optical density vs. total terpyridine concentration again traces a sigmoidal isotherm with a Hill coefficient of  $1.9 \pm 0.3$  (Figure 2b). Thus, for terpyridine, the activation isotherm shows essentially the same sigmoidicity as does the chelator binding isotherm. Note also that these data show that the sigmoidicity in the activation isotherm *does not* arise from the presence of contaminating metal ions.

**Identification of the Divalent Metal Ion Involved in the Chelator-Induced Activation of the 7S NGF Esteropeptidase.** 7S NGF binds zinc ion both with high affinity and with high specificity (Pattison and Dunn, 1975). However, the atomic emission spectrograph analysis of 7S NGF in 0.05 M Tris buffer, pH 7.4, indicates that several different metal ions (Fe, 1.9 ppm; Mn < 0.1 ppm; Cu, 1.0 ppm; Zn, 2.5 ppm; Mo, 0.2 ppm; Ni < 0.1 ppm) are present in more than trace amounts. Note that of the transition and near-transition metals detected, zinc is present at the highest concentration.

As shown in Figure 3a, and as discussed above, the spectrum produced by the interaction between 7S NGF and terpyridine exhibits two maxima, one at  $321.5 \pm 0.5$  nm and one at  $332.5 \pm 0.5$  nm. Figure 3b presents selected spectra for the complexes formed between terpyridine and those divalent metal ions that are shown by atomic emission spectroscopy to be present in the stock 7S NGF preparation. Of the divalent metal ion–terpyridine complexes that absorb in the same portion of the spectrum as the 7S NGF–terpyridine mixture (Hoyer et al., 1966) and that have been shown to be present in significant amounts by atomic emission spectroscopy, the spectrum produced by the bis(terpyridine)–zinc ion complex most closely fits both the position of the spectral maxima and the ratio of the intensities between the two 7S NGF–terpyridine spectral peaks (Figure 3a,b). Although the nickel–terpyridine complex also shows a similar spectrum, the metal ion analysis (above) indicates that nickel ion is present in an amount that is approximately 20-fold more dilute than zinc ion. Thus, there is present no more than 1 nickel ion/10–20 7S NGF molecules (based on the previously reported stoichiometry of 1–2 zinc ions/7S NGF, Pattison and Dunn, 1975). The fact that the 7S NGF–terpyridine mixture shows little or no absorbance above 400 nm, effectively rules out the possibility that divalent iron, which has a strong absorbance at 552 nm when complexed with terpyridine, is involved in the divalent metal ion inhibition of 7S NGF esterase activity.

Figure 4 compares the fluorescence emission spectra obtained respectively from the interaction of HQSA with native 7S NGF (trace C, upper set of spectra) to the fluorescence emission spectrum for the tris(HQSA)–zinc ion complex (trace C, lower set of spectra). Since the HQSA complexes with Cu(II), Ni(II), Co(II), Fe(II), or Mn(II) do not fluoresce, and since the fluorescence maxima ( $\lambda_{\text{ex}}$  360 nm) of the Ca(II)– and Mg(II)–HQSA complexes ( $\lambda_{\text{em}}$  500 nm) are greatly different, it is clear that the fluorescence spectrum of the 7S NGF–HQSA system arises from the formation of the tris-

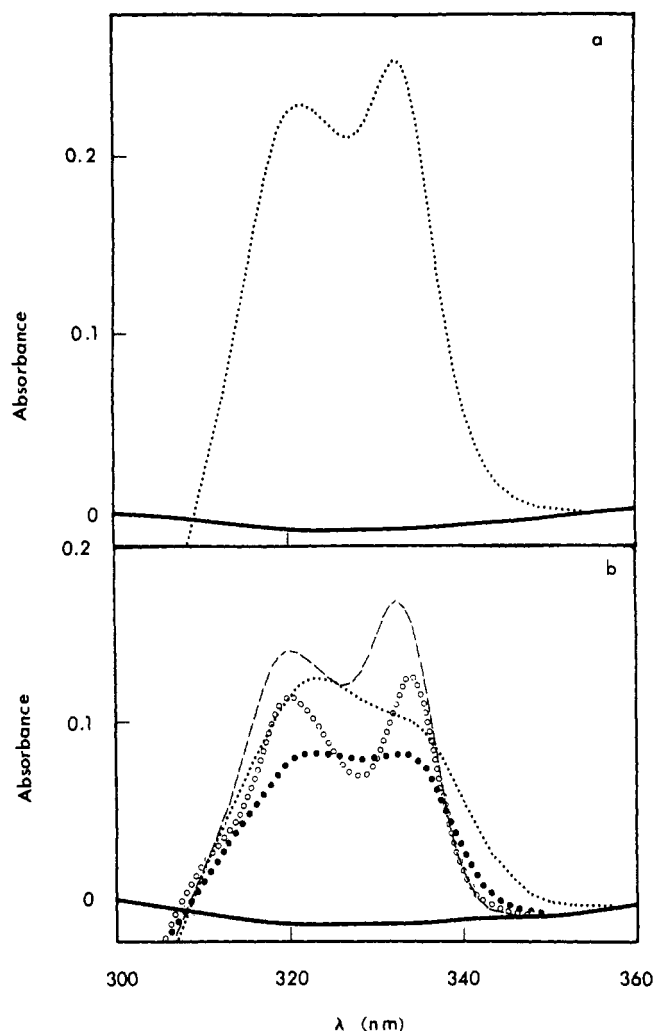


FIGURE 3: (a) The difference spectrum produced by the interaction between 2,2',2''-terpyridine and 7S NGF. This spectrum was recorded after a 90-min incubation of  $\sim 3 \mu\text{M}$  7S NGF with  $50 \mu\text{M}$  terpyridine in 0.05 M Tris buffer, pH 7.4, at room temperature. The cuvette used for this spectral study was presoaked in concentrated HCl for 30 min followed by a double-distilled water wash to remove trace divalent metal ion contaminants. The spectrum was obtained with a Cary 118c spectrophotometer (scan rate = 0.2 nm/s). (b) The difference spectra produced by the interaction between 2,2',2''-terpyridine and selected divalent metal ions. These spectra were recorded after a 10-min incubation of  $5 \mu\text{M}$   $\text{Me}^{2+}$  with  $50 \mu\text{M}$  terpyridine in 0.05 M Tris buffer, pH 7.4, at room temperature. The spectra were obtained with a Cary 118c spectrophotometer (scan rate = 0.2 nm/s). The divalent metal ions studied were as follows:  $\text{Mn}^{2+}$  (●);  $\text{Cu}^{2+}$  (···);  $\text{Ni}^{2+}$  (○);  $\text{Zn}^{2+}$  (---). Under these same conditions, neither 1 mM  $\text{Ca}^{2+}$  nor 1 mM  $\text{Mg}^{2+}$  produced a significant spectrum.

#### (HQSA)–zinc ion complex.<sup>2</sup>

**Kinetics of 7S NGF–Chelator Interaction.** The formation of the 321.5–332.5 nm absorbing species occurs via a two-step process when terpyridine reacts with 7S NGF. Each step corresponds to approximately one-half of the total spectral change. The fast step is complete in the time span required for mixing and placing the sample in the spectrophotometer (approximately 20 s). The time-course of the fast step, as mea-

<sup>2</sup> The fluorescence emission spectra of HQSA (trace b in Figure 4a,b) is quenched by these transition metal ions. Spectral comparisons were measured under the following conditions: divalent metal ion (as either the nitrate or chloride salt),  $\sim 33 \mu\text{M}$ ; HQSA, 0.33 mM;  $\lambda_{\text{ex}}$ , 360 nm, Tris buffer, pH 7.40 (0.05 M), and  $25.0 \pm 0.2^\circ\text{C}$ . Control studies, involving competition of these metal ions with zinc ion, demonstrate that significant (nearly stoichiometric) amounts of complex are formed under these conditions.

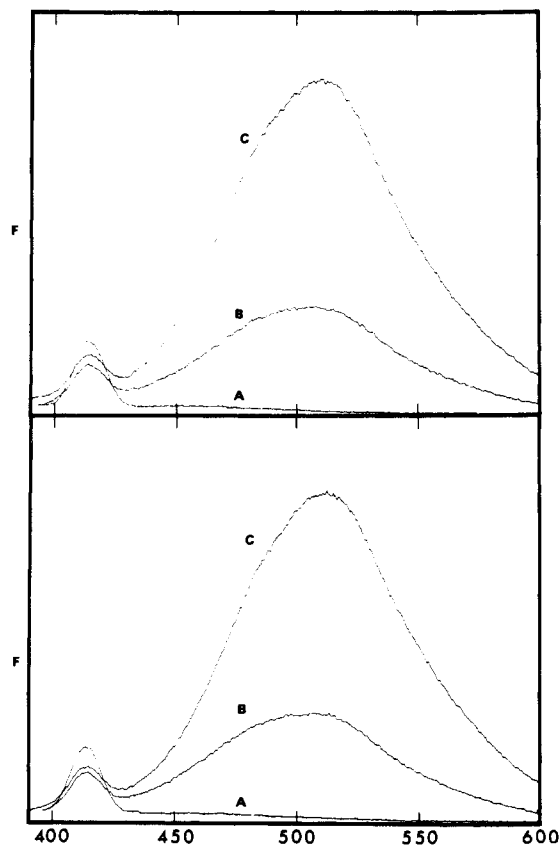


FIGURE 4: Comparison of the fluorescence emission spectrum obtained on incubation of native 7S NGF with 8-hydroxyquinoline-5-sulfonic acid (HQSA) (trace C, upper set) with the fluorescence emission spectrum of the Tris-HQSA-zinc ion complex (trace C, lower set). Traces A and B in both sets are respectively the instrument base line and the spectrum of HQSA in Tris buffer with no added divalent metal ion. Conditions, upper set of traces: (A) 0.05 M Tris buffer, pH 7.40; (B) addition of HQSA, 0.303 mM; (C) addition of 7S NGF,  $\sim 1.5 \mu\text{M}$ . Lower set of traces: (A) 0.05 M Tris buffer, pH 7.40; (B) addition of HQSA, 0.303 mM; (C) addition of  $\text{Zn}(\text{NO}_3)_2$ , 3.33  $\mu\text{M}$ . Instrument settings: slit bandwidths (excitation), 10 nm; (emission), 5 nm;  $\lambda_{\text{ex}}$ , 360 nm, sensitivity range, 0.03. (Note that the spectra are uncorrected.)

sured in a rapid-mixing stopped-flow apparatus is second-order overall, first-order with respect to 7S NGF and first-order with respect to chelator concentration. The slope of the best-fit straight line for the plot of  $k_{\text{obsd}}$  vs. [terpyridine] yields a second-order rate constant for this process of approximately  $1 \times 10^6 \text{ M}^{-1} \text{ s}^{-1}$ . This value was found to be indistinguishable from the rate constant for terpyridine binding to aquo-zinc ion under the same conditions of pH and buffer composition.

The second step observed in the reaction of terpyridine with 7S NGF is much slower, and the rate of this process can be measured in a conventional spectrophotometer. As noted above, this step accounts for approximately one-half of the total spectral change. This step adheres to a first-order rate law, and the apparent first-order rate constant ( $0.084 \text{ min}^{-1}$ ) was found to be independent of both chelator concentration and 7S NGF concentration over a fivefold range of concentrations ( $\sim 10$ – $50 \mu\text{M}$  for terpyridine, and  $\sim 0.1$ – $0.5 \text{ mg/ml}$  for 7S NGF) under conditions which produce maximal activation.

The time course of the fluorescence changes (viz. Figure 4) that accompany the reaction of HQSA with 7S NGF also is composed of more than one step. Conventional fluorescence emission kinetic studies show the occurrence of a rapid initial increase in fluorescence ( $\lambda_{\text{em}} \sim 520 \text{ nm}$ ) that is complete within the time required for mixing and placing the sample into

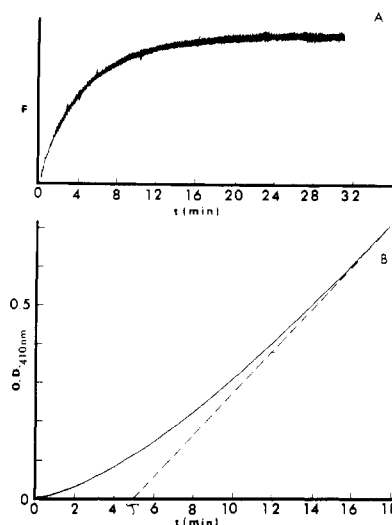


FIGURE 5: The traces in A and B compare the time course of the slow step for the fluorescence emission changes that accompany the reaction of 8-hydroxyquinoline-5-sulfonic acid (HQSA) with native 7S NGF (trace A) with the rate-of-change in the steady-state-rate of hydrolysis of the artificial substrate,  $\alpha$ -N-benzoyl-D,L-arginine-p-nitroanilide (BAPNA) (trace B) brought about by the reaction of HQSA with 7S NGF. Note in trace A that the fast phase of the fluorescence changes (see text) is not shown. In B, extrapolation of the final steady-state-rate process (---) back to zero product formation gives  $\tau$ , the reciprocal of the apparent first-order rate constant for the activation process (see text). Conditions: trace A; 0.303 mM HQSA,  $\sim 0.8 \mu\text{M}$  7S NGF, 0.05 M, pH 7.40, Tris buffer, and  $25.0 \pm 0.5^\circ \text{C}$ . Instrument settings:  $\lambda_{\text{ex}}$ , 360 nm;  $\lambda_{\text{em}}$ , 520 nm; slit bandwidths (excitation) 5 nm; (emission) 10 nm; sensitivity range, 0.01. Identical conditions were employed in trace B except that the reaction mixture also contains 1 mM BAPNA. The reaction in A was initiated by the addition of HQSA to the buffered 7S NGF solution. The reaction in B was initiated by the addition of native 7S NGF to the buffered HQSA-BAPNA solution.

the instrument ( $\sim 10 \text{ s}$ ). This rapid process is followed by a much slower increase in fluorescence. The slow step is an apparent first-order process,  $k_{\text{obsd}} = 0.20 \text{ min}^{-1}$  (see Figure 5A). The amplitude of the rapid fluorescence emission change (not shown) is approximately twice that associated with the slow step.

The rate of activation is defined as the rate-of-change of the slope of the progress curve for product appearance (Figure 5B). As the activation rate represents the rate-of-change of the steady-state rate of BAPNA hydrolysis with time, direct measurements of this rate have proved to be difficult. Thus, rather than attempt differentiation of the curve, an experimentally determined parameter,  $\tau$ , has been measured (see the Appendix of the following paper for the derivation of the expression for  $\tau$ ). This quantity is defined as the time value obtained from extrapolation of the final steady-state rate back to the abscissa intercept, as illustrated in Figure 5B. The  $\tau$  value is related to the rate constant(s) for the activation mechanism as defined in the Appendix of the following paper in this issue. Under the quasi-irreversible conditions employed in these kinetic studies, an apparent first-order activation rate constant ( $1/\tau$ ) of  $\sim 0.20 \text{ min}^{-1}$  is obtained (Figure 5B). Within the limits of experimental error, this value is found to be numerically identical with the apparent first-order rate constant for the slow, fluorescence emission change observed on reaction of HQSA with 7S NGF (Figure 5A). A similar correspondence is found between the rate of the slow step derived from the spectral changes that accompany the reaction of terpyridine with 7S NGF ( $0.10 \text{ min}^{-1}$ ) and the value of  $1/\tau$  for the activation process.

## Discussion

The fact that zinc copurifies with 7S NGF in approximately stoichiometric amounts (1–2 g-atoms of  $\text{Zn}^{2+}$ /mol of 7S NGF) indicates that 7S NGF has a high affinity for zinc ion (Pattison and Dunn, 1975). Furthermore, our previous studies have shown zinc ion to be a specific inhibitor for both the  $\gamma$ -subunit esteropeptidase ( $K_i \approx 8 \times 10^{-7}$  M) and the 7S NGF esteropeptidase. Finally, we have previously reported that divalent metal ion chelators cause activation of the 7S NGF esteropeptidase. These findings imply that activation of the 7S NGF esteropeptidase occurs via an interaction between the 7S NGF-bound zinc ion and divalent metal ion chelators. However, atomic emission spectroscopy analysis of a standard Tris-buffered 7S NGF solution indicates the presence of significant amounts of several divalent metal ions (i.e., Fe, Mn, Cu, Zn, Mo, Ni). Hence, these studies of the uv and the fluorescence emission spectral changes produced by the interactions of terpyridine or HQSA with 7S NGF bear directly on the identity of the divalent metal ion involved in the activation process as well as the mechanism of activation.

Terpyridine produces a 7S NGF esteropeptidase activation isotherm that is sigmoidal ( $n = 2.6 \pm 0.9$ , Figure 1). Concomitant with chelator-induced activation, terpyridine reacts with 7S NGF giving a characteristic uv spectrum (Figures 2 and 3). The optical density changes that characterize the major species (with maxima at  $321.5 \pm 0.5$  nm and  $332.5 \pm 0.5$  nm) trace a sigmoidal isotherm with a Hill coefficient ( $n = 1.9 \pm 0.3$ , Figure 2) that, within experimental error, is identical with the Hill coefficient derived from the terpyridine–7S NGF activation isotherm. The close similarity between the activation isotherm and the spectral titration curve strongly implies that the equilibrium interaction of terpyridine with 7S NGF that elicits esteropeptidase activation also elicits the observed spectral change.

Although it cannot be ruled out that protein interactions perturb the 7S NGF–terpyridine spectrum, the observed spectral band produced by terpyridine interaction with 7S NGF is virtually identical to the spectrum of the bis(terpyridine)–zinc ion complex (Figure 3). The fluorescence emission spectrum obtained on incubation of HQSA with native 7S NGF is identical to the fluorescence emission spectrum of the tris(HQSA)–zinc ion complex (Figure 4). Furthermore, the rate of formation of the tris(HQSA)–zinc ion complex is identical with the rate of formation of activated 7S NGF (Figure 5). These facts, taken together with the terpyridine studies, unambiguously establish (a) that zinc ion is the divalent metal ion involved in the chelator-induced activation process, and (b) that the chelator-induced activation process involves the sequestering of a 7S NGF-bound zinc ion. It is significant to note that the terpyridine–7S NGF uv spectrum corresponds to the formation of a bis(terpyridine)–zinc ion complex, while the HQSA–7S NGF fluorescence spectrum corresponds to the formation of a tris(HQSA)–zinc ion complex. It is unlikely that zinc ion in the bis(terpyridine) or tris(HQSA) complexes interacts directly with 7S NGF. Therefore, it is probable that chelator activation involves removal of the zinc ion from 7S NGF.

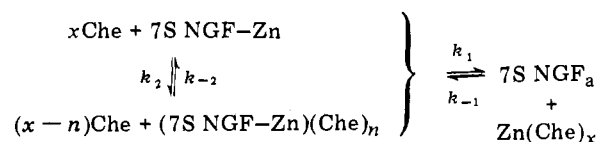
The identification of the observed spectral band with the formation of a bis(terpyridine)–zinc ion complex allows calculation of the zinc ion concentration (and the zinc ion/7S NGF ratio) if it is assumed that the 332.5-nm extinction coefficient for the bis(terpyridine)–zinc ion complex ( $\epsilon = 4.1 \times 10^4 \text{ M}^{-1} \text{ cm}^{-1}$ , Hoyer et al., 1966) is valid for the terpyridine–7S NGF system. Based on this value, a zinc ion to 7S

NGF ratio of  $1.50 \pm 0.50$  is estimated from these spectral studies. (A similar value is estimated from comparison of the relative intensity of the HQSA–NGF fluorescence emission spectrum with that of HQSA–zinc ion standards (viz. Figure 4). This value is essentially identical with the ratio determined by atomic absorption spectrometry (Pattison and Dunn, 1975).)

The fact that the terpyridine–7S NGF spectrum shows a small deviation from a true isosbestic point together with the fact that a minor spectral species ( $\lambda_{\text{max}} \approx 341$  nm) is observed at relatively low terpyridine concentrations (Figure 2) indicates that terpyridine interacts with more than one species in the 7S NGF solution. This heterogeneous chelator interaction is consistent with the emission spectrography data that indicate that more than one divalent metal ion species may be present in the 7S NGF solution. On the other hand, the fact that a 7S NGF–terpyridine spectral titration (Figure 2), recorded as the disappearance of free terpyridine absorbance at 290 nm, produces essentially the same sigmoidal isotherm (as when measured at 332 nm) is a strong indication that the amount of the minor species is insignificant relative to the amount of the principal species present.

A more complete picture of the activation process can be drawn from the biphasic time course observed for the reaction of terpyridine with 7S NGF. The initial, rapid spectral change is characterized by an apparent second-order rate constant that is similar in magnitude to the second-order rate constant for the reaction of terpyridine with the aquo zinc ion. Hence, the fast spectral change represents a relatively unhindered reaction of the chelator with 7S NGF-bound zinc ion that leads to no detectable esteropeptidase activation.

Although the second, slower reaction of chelator with 7S NGF also involves complex formation with the zinc ion, the reaction rate is independent of both the chelator and the 7S NGF concentrations. Since the rate constant for the spectral change is identical to the activation rate constant for either chelator, we conclude that activation occurs concomitant with the dissociation of the 7S NGF-bound zinc ion according to the sequence shown below:



where  $x$  and  $n$  are respectively the stoichiometry coefficients for chelator binding to zinc ion and to 7S NGF,  $a$  denotes the activated 7S NGF esteropeptidase. According to this scheme,  $\tau = 1/k_1$ , if  $[\text{Che}]_0 \gg [7\text{S NGF}]$  and if  $k_2[\text{Che}]$  and  $k_{-2} \gg k_1$  (see the Appendix to the following paper).

Moore et al. (1974) have proposed that the inhibition of the 7S NGF esteropeptidase activity arises from direct subunit–subunit interactions between the C-terminal Arg residues of the  $\beta$  subunits and the active sites of the  $\gamma$  subunits. In our previous paper (Pattison and Dunn, 1975), we presented indirect evidence that suggested that zinc ion was principally responsible for inhibition of the 7S NGF esteropeptidase. The spectral evidence presented in this paper demonstrates that chelator activation of the 7S NGF esteropeptidase is accomplished by removal of zinc ion from the protein. Conversely, zinc ion must be involved in the inhibition of the 7S NGF esteropeptidase activity.

## References

Barcroft, J., and Hill, A. V. (1909), *J. Physiol.* 39, 411.

- Cohen, S. (1960), *Proc. Natl. Acad. Sci. U.S.A.* **46**, 302.
- Frazier, W. A., Angeletti, R. H., and Bradshaw, R. A. (1972), *Science* **176**, 482.
- Greene, L. A., Shooter, E. M., and Varon, S. (1969), *Biochemistry* **8**, 3735.
- Holyer, R. H., Hubbard, C. D., Kettle, S. F. A., and Wilkins, R. G. (1966), *Inorg. Chem.* **5**, 622.
- Levi-Montalcini, R. (1966), *Harvey Lect.* **60**, 217.
- Levi-Montalcini, R., and Hamburger, V. (1953), *J. Exp. Zool.* **123**, 233.
- Moore, J. B., Mobley, W. C., and Shooter, E. M. (1974), *Biochemistry* **13**, 833.
- Pattison, S. E., and Dunn, M. F. (1975), *Biochemistry* **14**, 2733.
- Perez-Polo, J. R., Bamburg, J. R., DeJong, W. W. W., Straus, D., Baker, M., and Shooter, E. M. (1972), in *Nerve Growth Factor and its Antiserum*, E. Zaimis, Ed., London, Anthlone Press, p 19.
- Schenkein, I. (1972), *Handb. Neurochem.* **5B**, 503.
- Sillén, L. G., and Martell, A. D., Ed. (1964), *Chem. Soc., Spec. Publ.* **17**.
- Smith, A. P. (1969), Doctoral Thesis, Stanford University.
- Smith, A. P., Varon, S., and Shooter, E. M. (1968), *Biochemistry* **7**, 3259.
- Varon, S., Nomura, J., and Shooter, E. M. (1967), *Biochemistry* **6**, 2202.

## On the Mechanism of Divalent Metal Ion Chelator Induced Activation of the 7S Nerve Growth Factor Esteropeptidase. Thermodynamics and Kinetics of Activation<sup>†</sup>

Scott E. Pattison<sup>†</sup> and Michael F. Dunn\*

**ABSTRACT:** The 7S nerve growth factor protein (7S NGF) is a multisubunit zinc metalloprotein containing a masked trypsin-like esteropeptidase activity. Reaction of the native 7S NGF oligomer with divalent metal ion chelators effects an approximately sevenfold activation of the esteropeptidase activity via the sequestering and dissociation of the 7S NGF-bound zinc ion (Pattison, S. E., and Dunn, M. F. (1975), *Biochemistry* **14**, 2733; Pattison, S. E., and Dunn, M. F. (1976), *Biochemistry*, preceding paper in this issue). In this study, investigation of the relationship between chelator concentration and the extent of activation, as measured by the

steady-state rate of hydrolysis of  $\alpha$ -N-benzoyl-D,L-arginine-p-nitroanilide, has demonstrated that (a) the chelator-induced activation is a freely reversible process, (b) activated 7S NGF undergoes a slow loss of reversibility when incubated with chelator over long time-periods, (c) the affinity constant of 7S NGF for zinc ion is  $\sim 10^{10.5} \pm 10^{0.5} \text{ M}^{-1}$ , (d) chelator activation depends only on the ability of the chelator to sequester zinc ion, and (e) the activation process does not involve dissociation of the 7S oligomer to smaller subunit aggregates under conditions of low ionic strength.

The nerve growth factor protein (NGF)<sup>1</sup> promotes growth and differentiation of the noradrenergic neurons of the superior cervical ganglia and the sensory neurons of the dorsal root ganglia (see reviews by Levi-Montalcini, 1966; and Schenkein, 1972). The 140 000-dalton nerve growth factor (7S NGF) is an oligomeric protein consisting of three distinct classes of subunits,  $\alpha$ ,  $\beta$ , and  $\gamma$  (Smith et al., 1968). The  $\beta$  subunit contains the growth-promoting activity, while  $\gamma$  is a potent trypsin-like esteropeptidase which is inhibited while bound in the

oligomer (Greene et al., 1969). The existence of a stable oligomer (7S NGF) that appears to be no more biologically active in eliciting neurite outgrowth than one of its subunits ( $\beta$ ) in the in vitro organ culture assay (Varon et al., 1967) has raised questions concerning the functional significance of the  $\alpha$  and  $\gamma$  subunits. The objective of our studies has been to investigate the physical and enzymatic interactions between the  $\gamma$  enzyme and the  $\alpha$  and  $\beta$  subunits in 7S NGF in order to define the structural and functional properties of the oligomeric protein.

Our previous studies have established the following: (1) 7S NGF is a zinc metalloprotein, (2) zinc ion is a potent and specific inhibitor of both the native 7S NGF esteropeptidase and the  $\gamma$ -esteropeptidase ( $K_i \approx 8 \times 10^{-7} \text{ M}$ ) (Pattison and Dunn, 1975), and (3) zinc ion interacts directly with chelators during 7S NGF esteropeptidase activation (Pattison and Dunn, 1976).

In this paper, we establish (1) chelator activation of the 7S NGF esteropeptidase is a reversible phenomenon that appears to involve direct interaction of the chelator with zinc ion (and not subunit dissociation), (2) the affinity of 7S NGF for zinc ion is several orders of magnitude higher than the affinity of any of the isolated subunits for zinc ion, and (3) both ther-

<sup>†</sup> From the Department of Biochemistry, University of California, Riverside, California 92502. Received October 10, 1975. Supported by American Cancer Society Grants DT-4 (National Division) and 544 (California Division), and by funds from the University of California Cancer Research Coordinating Committee.

<sup>\*</sup> Present address: Institute of Molecular Biology, University of Oregon, Eugene, Oregon 97403. This work was carried out in partial fulfillment of the requirements for the Ph.D. degree and formed part of the dissertation.

<sup>1</sup> Abbreviations used are: NGF, nerve growth factor; BAPNA  $\alpha$ -N-benzoyl-D,L-arginine-p-nitroanilide; Tris, 2-amino-2-hydroxymethyl-1,3-propanediol; EDTA, ethylenediaminetetraacetic acid; CDTA, (trans-1,2-diaminecyclohexane)tetraacetic acid; OP, o-phenanthroline; NTA, nitrilotriacetic acid; BP, 2,2'-bipyridyl; MDA, N-methyliminodiacetic acid.